

advances.sciencemag.org/cgi/content/full/6/19/eaaz0571/DC1

Supplementary Materials for

CRISPR-based gene editing enables *FOXP3* gene repair in IPEX patient cells

M. Goodwin, E. Lee, U. Lakshmanan, S. Shipp, L. Froessler, F. Barzaghi, L. Passerini, M. Narula, A. Sheikali, C. M. Lee, G. Bao, C. S. Bauer, H. K. Miller, M. Garcia-Lloret, M. J. Butte, A. Bertaina, A. Shah, M. Pavel-Dinu, A. Hendel, M. Porteus, M. G. Roncarolo, R. Bacchetta*

*Corresponding author. Email: rosab@stanford.edu

Published 6 May 2020, *Sci. Adv.* **6**, eaaz0571 (2020)

DOI: [10.1126/sciadv.aaz0571](https://doi.org/10.1126/sciadv.aaz0571)

The PDF file includes:

Figs. S1 to S7
Tables S1 to S4

Other Supplementary Material for this manuscript includes the following:

(available at advances.sciencemag.org/cgi/content/full/6/19/eaaz0571/DC1)

Table S3

Supplementary Figures

Figure S1. The CRISPR system allows for precise *FOXP3* gene modification. (Corresponding to Figure 1) (A) Schematic representation of the edited *FOXP3* allele after HDR-mediated insertion of a cDNA encoding the alternatively spliced isoform of *FOXP3* lacking exon 2 (dE2, *FOXP3*^{dE2}, top construct). Construct includes the inserted *tNGFR* marker gene under the constitutive promoter, *PGK*, allowing marking of all edited cells. The *FOXP3* knockout allele (KO, *FOXP3*^{KO}, bottom construct) created by insertion of the *tNGFR* marker gene without a *FOXP3* cDNA. The *tNGFR* marker cassette flanked by polyadenylation signals (pA) to terminate mRNA processing and block expression of the downstream *FOXP3* gene elements, creating *FOXP3* knockout while marking edited cells. (B) The sequence of CRISPR sgRNA binding sites in exon 1 of the *FOXP3* gene relative to the start codon (red). The cut site of each sgRNA is underlined. The sgRNAs were tested either individually (sg1, sg2, sg3, and sg4) or as pairs (sg5&6 and sg7&8).

Figure S2. The *FOXP3* gene is precisely edited using CRISPR-mediated homology directed repair. (Corresponding to Figure 2) (A) Precise targeting of the *FOXP3* gene shown by an alternative in-out PCR strategy with forward primer (FP) in *tNGFR* and the reverse primer (RP) in the endogenous *FOXP3* gene outside of the 3' arm of homology. Band representing successful recombination observed from *FOXP3*^{FL} and *FOXP3*^{KO} gene edited HSPCs, both of which contain the *tNGFR* cassettes (adjacent lanes represent biological replicates). Control band targeting non-modified *FOXP3* region. (B) *FOXP3* editing rates by *tNGFR* in cord blood-derived HSPCs edited with *FOXP3*^{dE2} or *FOXP3*^{KO} constructs (mean \pm SD). (C) Comparison of editing frequency by two methods of detection: FACS for *tNGFR* and quantitative in-out PCR using Digital Drop PCR (ddPCR) (three *FOXP3*^{FLcoW} edited HSPC cell donors each tested in parallel by both methods). (D) Time course of *tNGFR* expression by flow cytometry on days post-editing, showing an initial *tNGFR* intermediate population that is resolved over time. (E) Off-target sites predicted bioinformatically using the COSMID tool. Pie chart of the gene region of the predicted off-target sites, showing the majority of sites (96%) in non-coding regions of the genome. (F) Ten off-target sites from GUIDE-seq oligo capture assay in U2OS cells with the closest gene name and number of sequencing reads per site. The *FOXP3* sgRNA (plus PAM) sequence shown above and mismatches with off-target sites are highlighted. The number of reads in the *FOXP3* on-target site shown for comparison.

Figure S3. Tregs and Teff cell populations are effectively separated prior to CRISPR-based editing. (Corresponding to Figure 3) (A) Purity of the fractionated Treg and Teff cell samples from peripheral blood shown by flow cytometry after anti-CD25 magnetic bead separation using two serial columns (CD25++). Representative flow cytometry plots showing the total population of CD4+ T cells prior to separation (left panel); Teff cell CD25- fraction (middle panel); and CD25++ Treg-enriched fraction (right panel) stained for Tregs in two parallel gating strategies. (B) Frequency of TSDR demethylated Tregs by epigenetic bisulfite qPCR. Shown are CD25- fraction after anti-CD25 magnetic bead separation enriched for Teff cells, CD25++ fraction enriched for Tregs, and MT-2 Treg cell line for comparison.

Figure S4. The *FOXP3* gene is knocked-in and knocked out using CRISPR-based homologous recombination. (Corresponding to Figure 3) (A) Example flow cytometry plot showing that MT-2 Tregs edited with the FL construct co-express *FOXP3* and *tNGFR*. Overlay contains negative control sample that is 98% double negative for *FOXP3* and *tNGFR* (*FOXP3*- *tNGFR*-), WT mock treated cells that are 98% *FOXP3*+ *tNGFR*-, and FL cDNA edited cells that are 93% double positive (*FOXP3*+*tNGFR*+). (B) Knockout of the *FOXP3* gene in the MT-2 Treg cell line by insertion of the *tNGFR* cassette without *FOXP3* cDNA into the *FOXP3* locus (*FOXP3*^{KO}). Shown is *FOXP3* protein expression by flow cytometry with median fluorescent intensity (MFI), comparing the wild-type MT-2 cells with two replicates of the *FOXP3*^{KO} treated cells.

Figure S5. Tregs edited with different constructs display comparable amounts of *FOXP3* function and *in vitro* suppressive capacity. (Corresponding to Figure 3) (A) *FOXP3* protein expression by flow cytometry in *FOXP3*^{dE2} edited Tregs compared with wild-type mock treated Tregs (mean \pm SD, n=2, p < 0.05). Data represented as the ratio of *FOXP3* median fluorescent intensity (MFI) relative to WT unmodified Tregs, showing roughly half expression (similar to full length cDNA expression). (B) Suppression assay comparing Tregs edited with cDNAs of the two *FOXP3* isoforms, *FOXP3*^{FLcoW} and *FOXP3*^{dE2}. The percent calculated suppression shown to the left. Graph to the right showing quantified suppressive capacity of three matched Tregs samples edited in parallel with the two constructs, showing that both isoforms support a similar level of

suppressive function in Tregs. (C) Suppression assay testing the function of Tregs from two healthy donors (HD) edited with *FOXP3*^{FL} and *FOXP3*^{FLcoW}. The calculated percent suppression of CFSE-labeled stimulated responders (R*) is shown to the left. As a negative control, cultured Teff cells from a parallel *FOXP3* editing experiment were used in place of Tregs and were shown to not be suppressive (N/A). (D) Suppression assay demonstrating that *FOXP3*^{FLcoW} edited Teff cells lack suppressive function as anticipated. The proliferation rate of stimulated responders (R*) is similar to that of responders co-cultured with WT mock treated or *FOXP3*^{FLcoW} edited Teff cells.

Figure S6. *FOXP3* gene editing preserves Teff cell proliferative function. (Corresponding to Figure 4) Time course of proliferation of Teff cells after activation with anti-CD3/28 beads (1:100 bead:cell ratio), showing progressive proliferation on subsequent days 2, 3, and 4 post-activation. Non-activated cells included for comparison and show some residual proliferation due to pre-editing activation and culturing. The wild-type Teff cells are compared to *FOXP3*^{FLcoW} edited Teff with no statistically significant differences observed (mean \pm SD, n=3, p = ns).

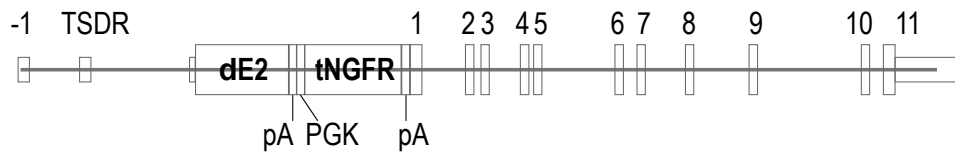
Figure S7. *FOXP3* edited HSPCs retain multi-lineage engraftment and differentiation potential. (Corresponding to Figure 6) (A) Phenotypic analysis of edited and control HSPCs pre-injection by flow cytometry, evaluating editing rates (tNGFR+), CD34+ purity, and different HSPC subsets including lymphoid-primed multipotent progenitors (LMPP, CD34+CD38-CD45RA+CD90-/v), multipotent progenitors (MPP, CD34+CD38-CD45RA-CD90-), and HSCs (CD34+CD38-CD45RA-CD90+). (B) Survival curve of mice engrafted with HSPCs from 3 experimental conditions over time. (C) Persistence of edited tNGFR+ cells engrafted in the hu-mouse at wk 14 demonstrated by flow cytometry. (D) Quantification of tNGFR+ rates in hu-mouse bone marrow at wk 14 showing different cord blood HSPC donors. (E) Genomic analysis showing percentage of cells with unmodified wild-type *FOXP3* alleles (blue), alleles edited by NHEJ and containing indel mutations (gray, TIDE analysis), and alleles edited by HDR (red, ddPCR in-out PCR). Shown is the genotype of HSPCs pre-injection (left) and in hu-mouse bone marrow at wk 14, demonstrating that *FOXP3* edited cells do not expand abnormally *in vivo*. (F) Functional testing of *in vivo*-differentiated CD4+ CD25- Teff cells sorted from the hu-mouse spleen. CFSE-stained Teff cells were stimulated with 1:100 and 1:25 b:c ratio using anti-CD3/28 beads and the proliferation rate was monitored by flow cytometry at day 4 post-stimulation. *FOXP3* edited Teff cells were sorted into tNGFR+ and tNGFR- fractions. Human peripheral blood-derived Teff cells were included for reference. (G) Suppression assay on CD4+CD25+ Tregs sorted from hu-mouse spleen. Flow cytometry plots of CFSE-stained responders stimulated with 1:25 b:c ratio. *FOXP3* edited Tregs were sorted into tNGFR+ and tNGFR fractions and co-cultured with responders.

Figure S1. The CRISPR system allows for precise *FOXP3* gene modification.

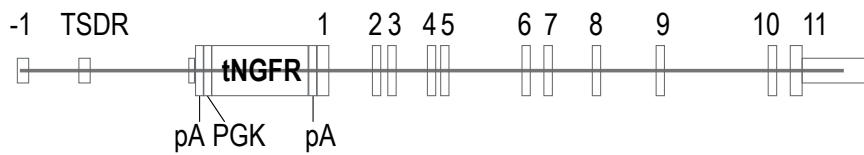
A

Alternative experimental constructs

Knock-in of alternatively spliced cDNA lacking exon 2 (*FOXP3*^{dE2})



Knockout of *FOXP3* by disruption with tNGFR maker gene (*FOXP3*^{KO})



B

CRISPR sgRNA Screen Target Sites in Exon 1

CCTGCCCTTGGACAAGGACCCG **ATG**CCCAACCCAGGCCTGGCAAGCCCTCGGCCCTTCCTTGGCCCTTGGCCCATCCCCAGGAGCCTCGCCAGCTGGA

E1_1 TTGGACAAGGACCCGATGCC

E1_2 AGGACCGATGCCAA CCCC

E1_3 AGGAGCCTCGCCAGCTGGA

E1_4 GGCAAGCCCTCGGCCCTTC

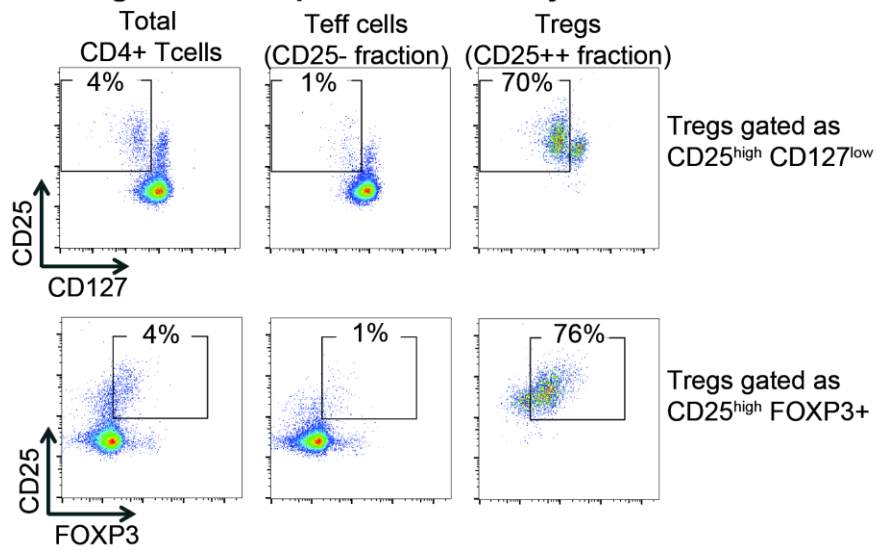
E1_5_6 GGCAAGCCCTCGGCCCTTC TTGGCCCTTGGCCCAT CCCC

E1_7_8 GGCTGGCAAGCCCTCGGCC CCCCAGGAGCCTCGCC CAGC



Figure S3. Tregs and Teff cell populations are effectively separated prior to CRISPR-based editing.

A Treg and Teff Separation and Purity



B Treg Purity by TSDR Demethylation

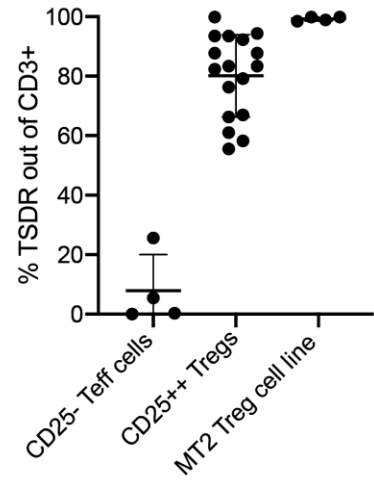


Figure S4. The *FOXP3* gene is knocked-in and knocked out using CRISPR-based homologous recombination.

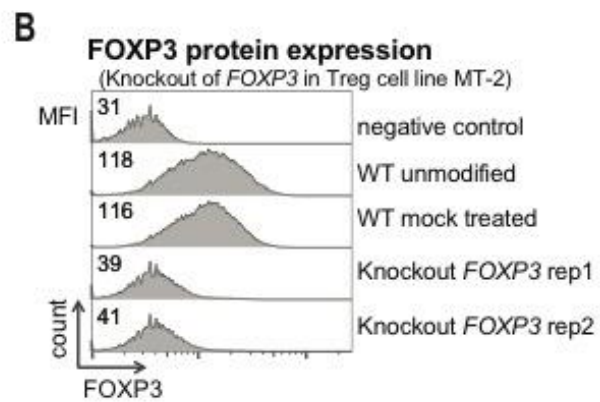
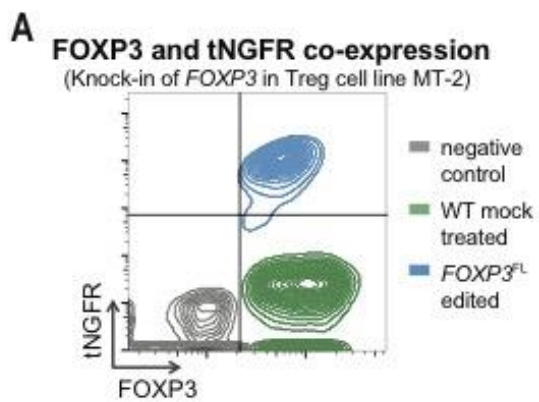


Figure S5. Tregs edited with different cDNA constructs display comparable amounts of FOXP3 function and *in vitro* suppressive capacity.

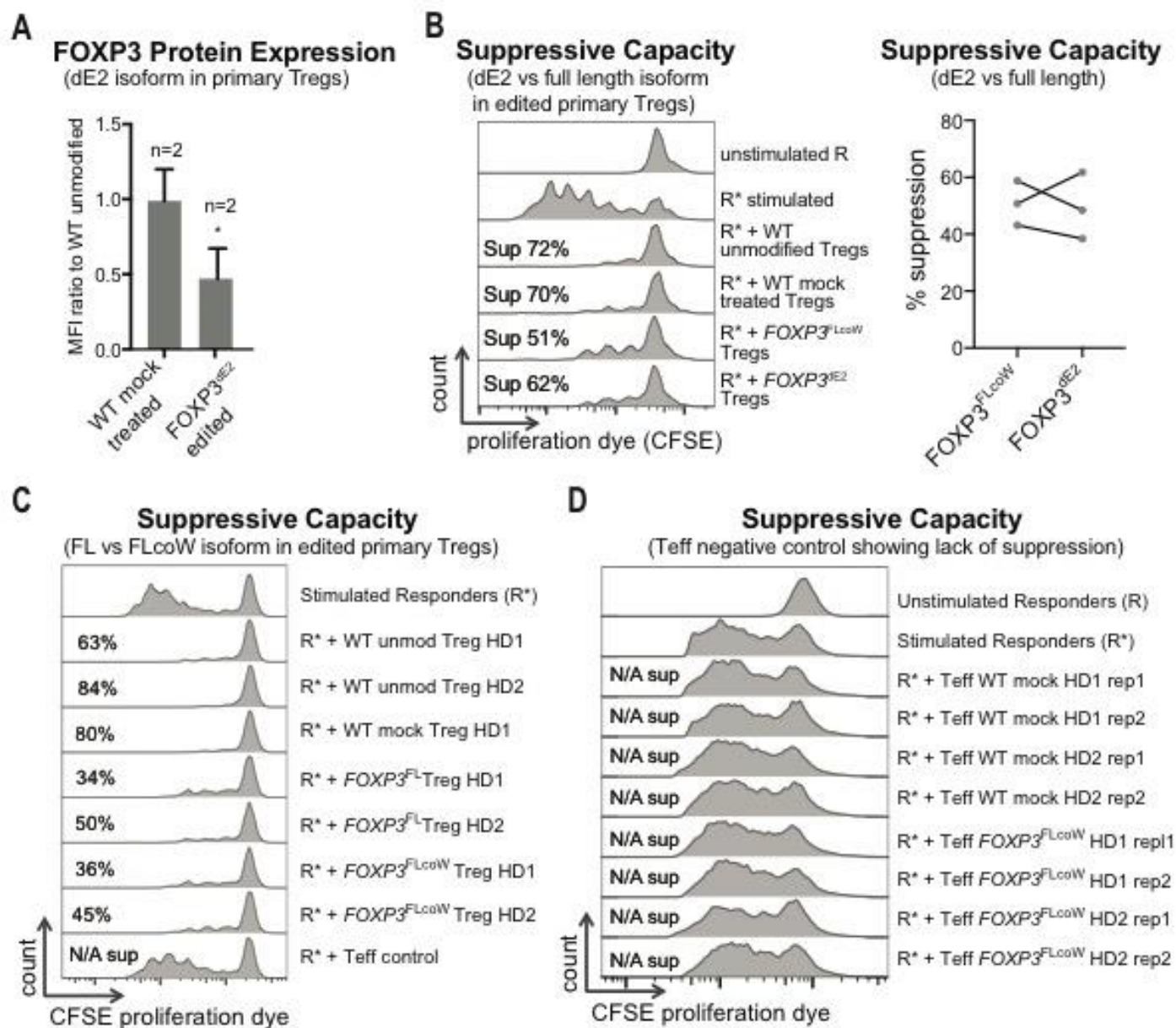


Figure S6. *FOXP3* gene editing preserves Teff cell proliferative function.

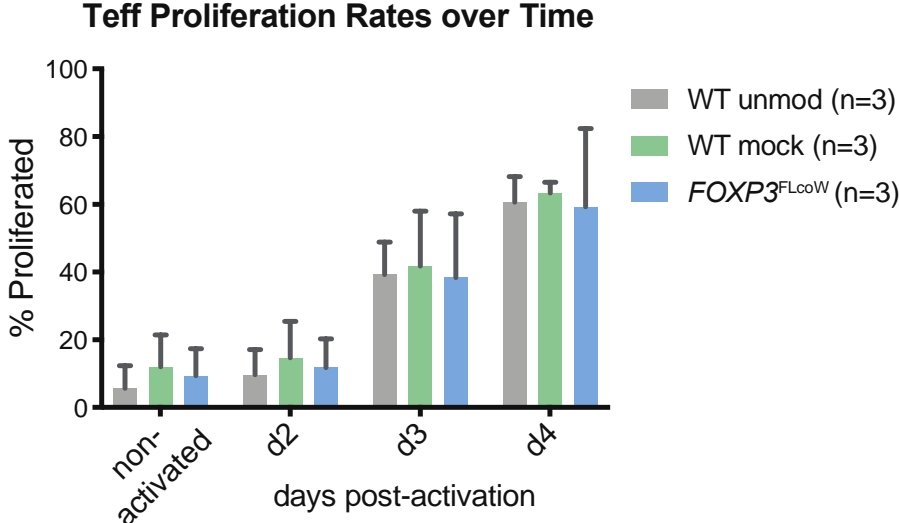
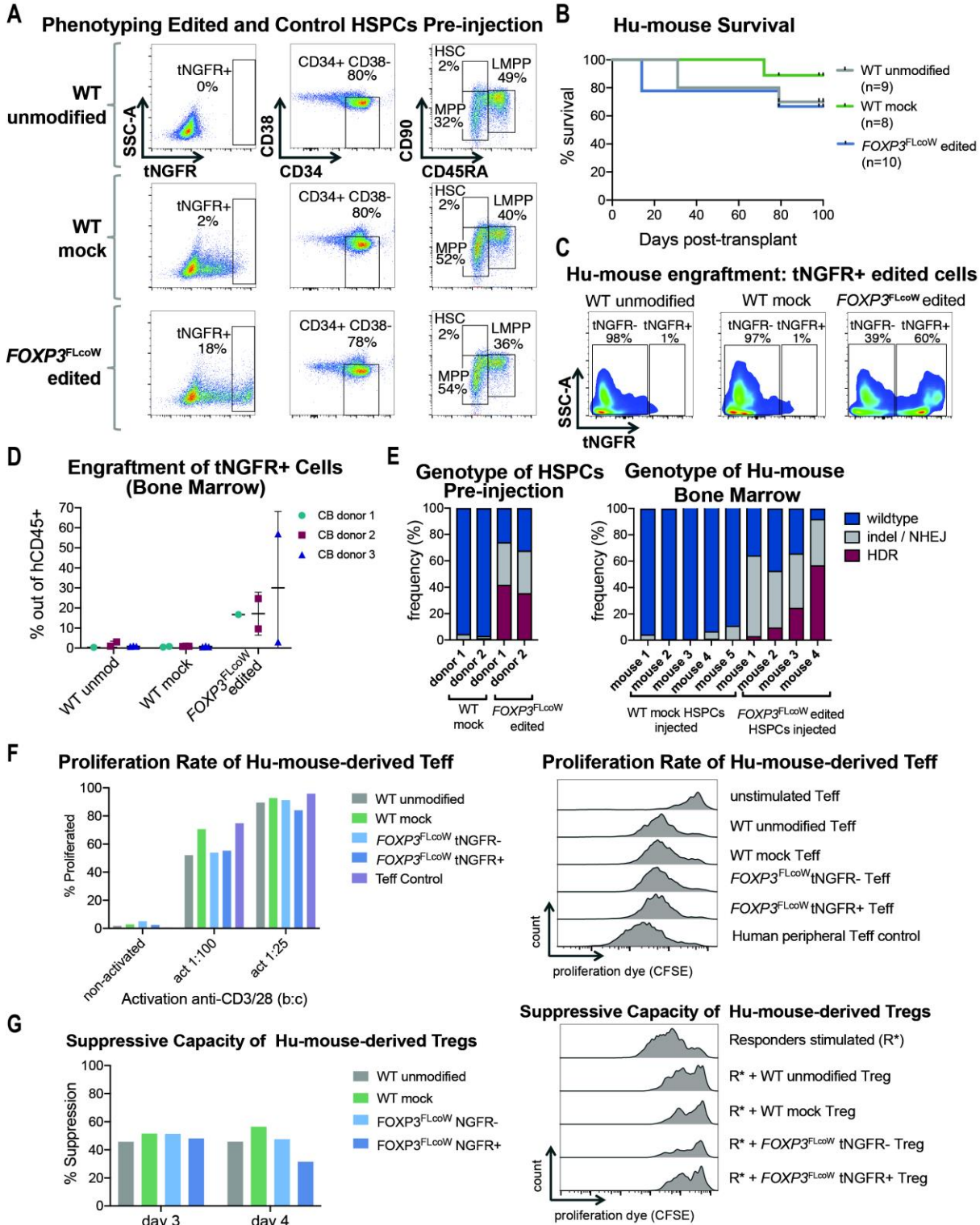


Figure S7. *FOXP3* edited HSPCs retain multi-lineage engraftment and differentiation potential.



Supplementary Materials:

Table S1. *FOXP3* sgRNAs, primers, and probes.

Assay	Name	Sequence
<i>FOXP3</i> sgRNAs used for screening	sgRNA_FOXP3_E1_1	5'-GGCATCGGGTCCTTGTCCAA-3'
	sgRNA_FOXP3_E1_2	5'-AGGACCCGATGCCCAACCCC-3'
	sgRNA_FOXP3_E1_3	5'-TCCAGCTGGGCGAGGCTCCT-3'
	sgRNA_FOXP3_E1_4	5'-GAAGGGGCGGAGGGCTTGCC-3'
	sgRNA_FOXP3_E1_5	5'-GAAGGGGCGGAGGGCTTGCC-3'
	sgRNA_FOXP3_E1_6	5'-TTGGCCCTTGGCCATCCCC-3'
	sgRNA_FOXP3_E1_7	5'-GGCCGAGGGCTTGCCAGGCC-3'
	sgRNA_FOXP3_E1_8	5'-CCCCAGGAGCCTCGCCCAGC-3'
Chemically modified sgRNA used for <i>FOXP3</i> editing	sgRNA_FOXP3_E1_2	5'- 2'OMe(A(ps)G(ps)G(ps))ACC CGA UGC CCA ACC CCG UUU UAG AGC UAG AAA UAG CAA GUU AAA AUA AGG CUA GUC CGU UAU CAA CUU GAA AAA GUG GCA CCG AGU CGG UGC UUU 2'OMe(U(ps)U(ps)U)-3' (ps indicates phosphorothioate, 2'OMe indicates 2'-O-methyl)
TIDE analysis primers for <i>FOXP3</i> indel rates	FP E1 TIDE FOXP3 RP E1 TIDE FOXP3	5'-CTAGAGCTGGGGTGCAACTATGG-3' 5'-GACTACAATACGGCCTCCTCCTCTC-3'
<i>FOXP3</i> in-out PCR primers for qualitative analysis of HDR	FOXP3_out5arm_FP FOXP3_cDNA_RP FOXP3_NGFR_FP FOXP3_out3arm_RP FOXP3_in3arm_control_FP FOXP3_out3arm_control_RP	5'-ATGTCAGCTCGGTCCTTCCA-3' 5'-TGGCATAGGATTAAGGGAAGT-3' 5'-AGCCTTCAAGAGGTGGAACA-3' 5'-AGGCCATCCTGATCCTCAC-3' 5'-TGCCTCCTCTTCTTCTTGA-3' 5'-GAGCCTCGAAAACCCTGACT-3'
<i>FOXP3</i> in-out PCR primers and probes for quantitative ddPCR analysis of HDR	FOXP3_inNGFR_ddPCR_FP FOXP3_inside_probe_FAM FOXP3_out3arm_ddPCR_RP FOXP3_control_ddPCR_FP FOXP3_control_probe_HEX FOXP3_control_ddPCR_RP	5'-GGGAGGATTGGGAAGACAAT-3' 5'-TCAGAGATTGGAGGCTCTCC-3' 5'-ACAATACGGCCTCCTCCTCT-3' 5'-CACCGAAATCGGTATTAGTTTG-3' 5'-CAGTTCTGGAGGCCAGAGTC-3' 5'-CCCGGGGGAGTATAGAAGG-3'
Sequencing of <i>FOXP3</i> locus and mRNA expressed from edited allele	FOXP3_E-1_FP2 FOXP3_E5_RP2 FOXP3_E5_RP2d FOXP3_E1_FP1d FOXP3_E3_RP1d FOXP3_E2_FP3d FOXP3_E5_FP4d FOXP3_E10_RP4d FOXP3_E11_RP1d FOXP3_E11_RP2d FOXP3_E11_FP1d FOXP3_NGFR_RP1 FOXP3_E11_FP2d FOXP3_NGFR_RP2 FOXP3_E10_FP1d FOXP3_NGFR_RP3	5'-CCAGGCTGATCCTTTTCTGTCA-3' 5'-CAGACACCATTGCCAGCAG-3' 5'-CAGACGCCATTGGCCAGAAGG-3' 5'-TGCACCCAAGGCTTCTGAC-3' 5'-CTGGAGAAGTGGGGTCC-3' 5'-CGCCCTCATTTTCATGCACCA-3' 5'-TTGAAGAGCCAGAAGATTTC-3' 5'-ATGCGAACATTCTTGTGAAC-3' 5'-AGCACTTGTGCAGGGAAAGA-3' 5'-CCCGGCGTGGGATTGCTGCA-3' 5'-AACGGTCACAAAGACCAAGC-3' 5'-CACCGCTGTGTGTGTACAGG-3' 5'-AACGCTATTTCGGCACAATCT-3' 5'-CCAGTCGTCTCATCCTGGTAG-3' 5'-AGGCACCTGAGAAGCAAAGA-3' 5'-GCTCACACACGGTCTGGTT-3'

FOXP3_E10_FP2d	5'-AGGCACCTGAGAAGCAAAGA-3'
FOXP3_E1_RP1	5'-GGGGTTCAAGGAAGAAGAGG-3'
FOXP3_E11_FP3d	5'-AACGGTCACAAAGACCAAGC-3'
FOXP3_E2_RP1	5'-CCTGGAGGAGTGCCTGTAAG-3'
FOXP3_E11_FP4d	5'-ACGCTATTCGGCACAATCTT-3'
FOXP3_E2/3_RP1	5'-TTGAGAGCTGGTGCATGAAA-3'
FOXP3_E-1_FP3	5'-ACCGTACAGCGTGGTTTTTC-3'
FOXP3_E7_RP1d	5'-TTGGTGAGAGCCATTTTTCC-3'
FOXP3_E-1_FP4	5'-AGAGAGAGGTCTGCGGCTTC-3'
FOXP3_E9_RP1d	5'-GAGGCCTCATGTTGTGGAAT-3'
FOXP3_E7_FP1d	5'-GGAAAAATGGCTCTCACCAA-3'
FOXP3_E6_RP1d	5'-CCAACAAGTGGTCTGCTTGA-3'
FOXP3_E-1_RP1	5'-AGGCTTGGTGAAGTGGACTG-3'
FOXP3 E1_RP2d	5'-GGCTAGGTGCGCTAGGTTTT-3'

Table S2. Off-target site analysis of FOXP3 CRISPR system. See extended off-target analysis (including other sgRNAs screened) in attached supplementary data file.

Method	OT	Predicted OT?	Sequence	Gene region	Genome location (hg19)	Nearest gene	Notes
NGS validation in BM	OT1_NGS	OT1_B	TGGCACCGATGC CCAACCCCTGG	Intron 3	chr15:90449230-90449252	ARPIN	0.6% / 1.6% CB/BM
	OT2_NGS	OT3_B	AGGACCAGATGC CCAACACCTGG	intergenic	chr6:28980904-28980926	ZNF311	0.4% / 0.8% CB/BM
	OT3_NGS	OT4_B	CTGTCCCCATGC CCAACCCAGG	intron 2	chr6:29638299-29638321	MOG	0.1% / 0.2% CB/BM
	OT4_NGS	OT14_B	AGGACACGAAGC CCAGCCCCGGG	In-RNA	chr17:43325321-43325343	MAP3K14-AS1	0.1% / 0.2% CB/BM
GUIDE-Seq in U2OS cells	OT1_GS	OT3_B	AGGACCAGATGC CCAACACCTGG	Intergenic	chr6:28980904-28980926	ZNF311	762 seq reads (vs 2155 in FOXP3)
	OT2_GS	Not predicted	AGGACCCCTAGC TCAACCCAGG	Intergenic	chr3:86673099-86673121	LINC02070	132 seq reads
	OT3_GS	Not predicted	AGGACCCAGACC CAACCCCTGG	Intergenic	chr12:30542757-30542778	IPO8	83 seq reads
	OT4_GS	OT8_B	AGCACCCGACCC CCAACCCAGG	Intergenic	chr16:11581470-11581492	LOC101927131	57 seq reads
	OT5_GS	OT13_B	AAGACCCGAAGC CCAGCCCCTGG	Exon	chr22:21383175-21383197	SLC7A4	54 seq reads
	OT6_GS	OT1_B	TGGCACCGATGC CCAACCCCTGG	Intron	chr15:90449230-90449252	ARPIN	48 seq reads
	OT7_GS	OT14_B	AGGACACGAAGC CCAGCCCCGGG	Exon	chr17:43325321-43325343	MAP3K14-AS1	27 seq reads
	OT8_GS	OT36_B	AGGCCCTGATGC CCAACCCAGG	Intron	chr19:45731177-45731199	EXOC3L2	20 seq reads
	OT9_GS	OT32_B	AGGACCCAGCC CAACCCCTGG	Intron	chr2:241677688-241677709	KIF1A	8 seq reads
	OT10_GS	Not predicted	AGGGATCCGTGC CCAACCCAGG	Intron	chr8:22409581-22409603	SORBS3	3 seq reads
Bioinformatic prediction by COSMID	OT1_B	OT1_B	TGGCACCGATGC CCAACCCCTGG	intron	chr15:90449230-90449252	ARPIN	score: 0.36
	OT2_B	OT2_B	TGCACCTGATGC CCAACCCAGG	intron	chr9:36896036-36896058	MIR4476	score: 0.38
	OT3_B	OT3_B	AGGACCAGATGC CCAACACCTGG	Intergenic	chr6:28980904-28980926	ZNF311	score: 4.23
	OT4_B	OT4_B	CTGTCCCCATGC CCAACCCAGG	intron	chr6:29638299-29638321	MOG	score: 0.57
	OT5_B	OT5_B	AGGCCCTGAAGC CCAACCCGGG	intron	chr11:8796275-8796297	LOC102724784	score: 0.9
	OT6_B	OT6_B	TGAACCCAATCC CCAACCCGGG	Intergenic	chr21:43451894-43451916	ZNF295	score: 1.12
	OT7_B	OT7_B	CGCACCCAATCC CCAACCCAGG	intron	chr16:55807075-55807097	CES1P1	score: 1.12
	OT8_B	OT8_B	AGCACCCGACCC CCAACCCAGG	Intergenic	chr16:11581470-11581492	LOC101927131	score: 1.35
	OT9_B	OT9_B	AGGACCTGAGGC CAAACCCAGG	Intergenic	chr4:153104124-153104146	LOC100996286	score: 2.03

OT10_B	OT10_B	TGGACCACATGC CCCACCCCTGG	intron	chr1:234767750- 234767772	LINC00184	score: 2.4
OT11_B	OT11_B	GGGACTCGAAGC CCCACCCCTGG	intron	chr19:17955771- 17955793	JAK3	score: 2.61
OT12_B	OT12_B	TGCACCCCATGC CCAGCCCCAGG	intron	chr11:44917438- 44917460	TP53I11	score: 2.72
OT13_B	OT13_B	AAGACCCGAAGC CCAGCCCCCTGG	TTS	chr22:21383175- 21383197	SLC7A4	score: 2.93
OT14_B	OT14_B	AGGACACGAAGC CCAGCCCCGGG	promoter	chr17:43325321- 43325343	MAP3K14	score: 3.01
OT15_B	OT15_B	AGGACCTGAGGC CCAGCCCCAGG	TTS	chr14:10061074 4-100610766	DEGS2	score: 3.03
OT16_B	OT16_B	TGGACCCCAAGC CCAGCCCCAGG	promoter	chr6:31746006- 31746028	VWA7	score: 3.07
OT17_B	OT17_B	GGGCCCCGATCC CCAGCCCCCTGG	intron	chr6:167070257- 167070279	RPS6KA2	score: 3.17
OT18_B	OT18_B	CGGGCCCGATG CGCATCCCCGGG	exon	chr11:64645666- 64645688	EHD1	score: 3.57
OT19_B	OT19_B	GGGACCCCATCC CCAAGCCCAGG	intron	chr3:129308525- 129308547	PLXND1	score: 3.97
OT20_B	OT20_B	GGGACCCCATGC TCAAGCCCAGG	intron	chr9:140864656- 140864678	LOC105376331	score: 4.37
OT21_B	OT21_B	GGGACCCGCTG CCCTGCCCCGG G	Intergenic	chr14:10200722 0-102007242	DIO3OS	score: 4.55
OT22_B	OT22_B	GGGACCCCATGC CCGAGCCCCGG	promoter	chr17:2240485- 2240507	TSR1	score: 5.17
OT23_B	OT23_B	GGGACCTGATGC CCAGGCCAGG	intron	chr1:2180639- 2180661	SKI	score: 5.53
OT24_B	OT24_B	TGGCCCCGATTC CCAACCACAGG	intron	chr4:7805378- 7805400	AFAP1	score: 5.87
OT25_B	OT25_B	GGGTCCCGATGC TCAACCACGGG	intron	chr4:62330745- 62330767	ADGRL3	score: 6.27
OT26_B	OT26_B	AGGTCCCCATGC CCAACCACGG	intron	chr1:37493536- 37493558	GRIK3	score: 6.44
OT27_B	OT27_B	GGGACCCAATGC CCAGCACCTGG	Intergenic	chrX:150516968 -150516990	VMA21	score: 6.57
OT28_B	OT28_B	GGGACCCCATGC ACAACCCAAGG	intron	chr6:144284337- 144284359	PLAGL1	score: 7.37
OT29_B	OT29_B	TGGACCCCATGC CCAGCCTCAGG	non coding intron	chr20:411775- 411797	RBCK1	score: 7.57
OT30_B	OT30_B	CGGACCCGAAGC CCAAGCCTAGG	intron	chr3:47866410- 47866432	DHX30	score: 9.5
OT31_B	OT31_B	GGGACCCGATGC CCAAGCCTGG	Intergenic	chr2:121115594- 121115615	INHBB	score: 7.51
OT32_B	OT32_B	AGGACCCAGCC CAACCCCTGG	intron	chr2:241677688- 241677709	AQP12A	score: 1.28
OT33_B	OT33_B	GGGATCCGTGCC CAACCCAGG	intron	chr8:22409582- 22409603	SORBS3	score: 1.05
OT34_B	OT34_B	GGGACCCGATTG CCCACCCCTGG	Intergenic	chr7:53287356- 53287379	POM121L12	score: 3.5
OT35_B	OT35_B	TGGACCCGCATG GCCAACCCAGG	Intergenic	chr16:50485999- 50486022	BRD7	score: 1.85
OT36_B	OT36_B	AGGCCCTGATGC CCAACCCAG	intron	chr19:45731177- 45731199	EXOC3L2	score: 0.4
OT37_B	OT37_B	CAGCCCAGATGC CCAACCCAAG	exon	chr12:53800454- 53800476	AMHR2	score: 0.53
OT38_B	OT38_B	TGAACACCATGC CCAACCCAAG	intron	chr6:403206- 403228	IRF4	score: 0.63
OT39_B	OT39_B	GGGAATCCATGC CCAACCCAG	intron	chr22:38668168- 38668190	TMEM184B	score: 0.67
OT40_B	OT40_B	AGTACCCATTGC CCAACCCAG	intron	chr16:8622029- 8622051	TMEM114	score: 0.77
OT41_B	OT41_B	AGGAGCTGTTGC CCAACCCAAG	intron	chr5:149127157- 149127179	MIR378A	score: 0.77
OT42_B	OT42_B	GGGACAGGAGG CCCAACCCAG	intron	chrX:149940578 -149940600	MTMR1	score: 0.94
OT43_B	OT43_B	GGGACCCAACGA CCAACCCAG	Intergenic	chrX:58316356- 58316378	ZXDA	score: 1.57
OT44_B	OT44_B	AGGTCCCGGTGC CCTACCCAG	Intergenic	chr14:10305780 4-103057826	RCOR1	score: 2.42
OT45_B	OT45_B	AAGACTCGATGC CCAGCCAG	intron	chr7:94943990- 94944012	PON1	score: 2.64
OT46_B	OT46_B	GGGGCCGGATG CCCAGCCAG	3'UTR	chr19:2273114- 2273136	OAZ1	score: 2.7
OT47_B	OT47_B	AGGAACTGATGC CCACCCCAAG	intron	chr8:32427315- 32427337	NRG1	score: 2.72

OT48_B	OT48_B	GGGGCCCGAGG CCCACCCCTAG	Intergenic	chr7:156833005- 156833027	MNX1	score: 2.97
OT49_B	OT49_B	GGGACCAGAAGC CCAGCCCCCAG	Intergenic	chr8:115530370- 115530392	CSMD3	score: 3.03
OT50_B	OT50_B	TGGACCCAATCC CCATCCCCAAG	intron	chr12:11109736 1-111097383	HVCN1	score: 3.27
OT51_B	OT51_B	GGGAACAGATGC CCAAACCCAG	Intergenic	chr17:11123959- 11123981	SHISA6	score: 3.42
OT52_B	OT52_B	AGGACCAGAAGC CCAACCCAG	intron	chr7:74482748- 74482770	RCC1L	score: 4.73
OT53_B	OT53_B	TGGACCAGATGC ACAACCACAAG	Intergenic	chr3:162436725- 162436747	LINC01192	score: 6.33
OT54_B	OT54_B	CGGCCCCGATGC CCAGCTCCGAG	Intergenic	chr11:71350468- 71350490	KRTAP5	score: 6.47
OT55_B	OT55_B	GGGACCCAATGC CCCACCACAG	Intergenic	chr7:2541942- 2541964	LFNG	score: 7.17
OT56_B	OT56_B	GGGACCCGATGC CCCTGCCCAAG	unknown	chrUn_gl000228: 20563-20582	unknown	score: 7.2
OT57_B	OT57_B	GGGACCCGAAG CCCAAGACCCAG	Intergenic	chr11:68876144- 68876166	MIR3164	score: 7.5
OT58_B	OT58_B	CGGACCCGGTG CCCACCCTCAAG	Intergenic	chr16:88463639- 88463661	ZNF469	score: 7.65

Table S4. IPEX patient clinical data and FOXP3 mutations. Patients (ID*) 37, 64, 65, 77, and 78 were enrolled at the Stanford Center for Genetic Immune Diseases (CGID). Frequency of demethylated TSDR Tregs (**) in peripheral blood (out of CD3+ T cells) determined by bisulfite qPCR. Healthy donor range is 4.8±1.7% for males (mean ± standard deviation). IPEX patients often have above average frequency of mutated Tregs by testing of TSDR demethylation thought to be attributed to a compensatory mechanism.

Patient ID*	Mutation	Molecular outcome	Age	Clinical manifestations	Tregs (%)**	Treatment	Outcome	Notes
24	c.210+1 G>C	Exon 1 aberrant skipping, mRNA without start codon, reduced protein translation	At onset: 6yr; At blood draw: 12-13 yrs.	Gastritis, inflammatory gastropathy with ulcers, failure to thrive	9.2	Rapamycin for 3 years, followed by HLA-matched unrelated donor hematopoietic stem cell transplantation (MUD-HSCT, at age 14yr); steroids temporarily administered to treat oral aphthae	Rapamycin allowed clinical remission with latent inflammation of gastric mucosa histologically evident; HSCT allowed clinical remission while histology is still under evaluation	Published in Barzaghi <i>et al.</i> , <i>JACI</i> 2018 (4) and Passerini <i>et al.</i> , <i>JACI</i> 2019 (27)
37	c.1150G >A	Ala>Thr amino acid change in the forkhead domain, which might affect DNA binding; mutant FOXP3 protein expressed	At onset: 2 months; At blood draw: 26 yrs.	Chronic autoimmune enteritis, T1D, eczema, alopecia	12.8	Steroids, Tacrolimus, Azathioprine, Rapamycin, Humira	Partial disease control	Published in Barzaghi <i>et al.</i> , <i>JACI</i> 2018 (4)
64	c.1270_1 272delin sC	Frameshift mutation predicted to cause new C-terminal and misfolded protein degradation; absent FOXP3 protein expression	At onset: 2 wks; At blood draw: 4-12 mo	Autoimmune enteritis, dehydration, malabsorption, hyper IgE, eczema	13.1	Rapamycin, steroids; at 5mo he received an alpha,beta-cell depleted paternal haploidentical stem cell transplant.	Mixed donor chimerism in disease clinical remission (and low dose Rapamycin)	Younger brother of patient 65
65	c.1270_1 272delin sC	Frameshift mutation predicted to cause new C-terminal and misfolded protein degradation; absent FOXP3 protein expression	At onset: 1 mo; At blood draw: 12-16 mo	Chronic severe autoimmune enteritis, bowel obstruction, rectal bleeding, abdominal pain, malabsorption, weight loss, autoimmune hepatitis, eczema	31.6	Steroid, Tacrolimus, Ciclosporin, Campath, Rapamycin, followed by alpha,beta-cell depleted paternal haploidentical stem cell transplant at 18 months.	Full donor chimerism and normal immune reconstitution.	Older brother of patient 64

77	c.1129C>G	His>Asp amino acid change in the forkhead domain, which might affect DNA binding; mutant FOXP3 protein expressed	At onset: 13 yrs.; At blood draw: 14-15 yrs.	Inflammatory colitis, T1D, moderate eczema	4.5	Systemic or local steroids as needed	Recurrent moderate clinical manifestations	Older brother of patient 78 with milder presentation
78	c.1129C>G	His>Asp amino acid change in the forkhead domain, which might affect DNA binding; mutant FOXP3 protein expressed	At onset: infancy; At blood draw: 7 yrs.	Gastritis, colitis, arthralgias, failure to thrive	7.0	Steroids, Sulfasalazine, Azathioprin during recurrence	Recurrent moderate clinical manifestations	Also has two variants in <i>LRBA</i> gene [c.3905C>T(p.Thr1302Ile) and c.7675G>T(p.Ala2559Ser)]